



International Journal of Maritime Technology

Journal homepage: ijmt.ir



Parametric Assessment of Hull Geometry Effects on the Coupled Dynamics of Semi-Submersible Floating Wind Turbines

Mohammad Javad Eslahi ¹ , Saeid Kazemi ^{2*} , Mojtaba Ezam ³ , Majid Ghodsi Hasanabad ⁴ 

¹ Ph.D. student, Department of Civil Engineering, SRBIU, Tehran, Iran; mj.eslahi@srbiau.ac.ir

² Assistant Professor, Department of Civil Engineering, SRBIU, Tehran, Iran; saeid.kazemi@srbiau.ac.ir

³ Assistant Professor, Department of Physics Oceanography, SRBIU, Tehran, Iran; ezam@srbiau.ac.ir

⁴ Assistant Professor, Department of Mechanical Engineering, SRBIU, Tehran, Iran; ghodsi@iau.ir

ARTICLE INFO

Article History:

Received: 5 Feb 2026

Last modification: 5 Jun 2026

Accepted: 8 Jun 2026

Available online: 9 Jun 2026

Article type:

Research paper

Keywords:

Floating offshore wind Turbines

Coupled Dynamics

Hull Form Effects

Time-Domain Solution Method

Response Amplitude Operation

ABSTRACT

This study presents a systematic investigation into the influence of geometric parameters and structural characteristics on the dynamic response of a semi-submersible platform supporting a floating wind turbine, with an emphasis on identifying stable performance regimes rather than determining a single optimal configuration. The analyses initiated with preliminary linear evaluations and were subsequently complemented by nonlinear time-domain simulations. A comparison of these approaches demonstrates that while the linear model is useful for identifying general response trends, it fails to fully capture oscillation amplitudes or the coupling intensity among degrees of freedom, particularly under hydrodynamic nonlinearities and mooring system effects. Consequently, a realistic assessment of system behavior necessitates nonlinear analysis. The investigation focused primarily on surge, heave, and pitch motions, as sway, roll, and yaw contributed minimally to the global response. Results indicate that the vertical and rotational motions of the platform are governed not only by the heave plate geometry but also by its interaction with the offset column arrangement. Variations in heave plate diameter and thickness, in conjunction with the geometric configuration of the offset columns, alter the dynamic response by modifying the added mass, hydrodynamic damping, and the relative positions of the centers of gravity and buoyancy. Within the examined range, heave plate diameters of 24–30 m and thicknesses equivalent to 7–10.5% of the offset column height produced more stable responses without shifting natural frequencies toward resonance. Specifically, a diameter of approximately 28.5 m and a thickness of around 8% yielded balanced surge, heave, and pitch responses. However, comparable performance across adjacent configurations suggests a robust design envelope rather than a single unique optimum. Overall, the findings highlight the utility of evaluating geometric parameters within an integrated framework to elucidate the relationships between platform geometry, hydrodynamic coefficients, and the coupled dynamic response.

ISSN: 2645-8136



DOI:

Copyright: © 2025 by the authors. Submitted for possible open access publication under the terms and conditions of the Creative Commons Attribution (CC BY) license [<https://creativecommons.org/licenses/by/4.0/>]

1. Introduction

The growing global reliance on fossil fuels has not only intensified the energy crisis but has also led to substantial environmental degradation and increased greenhouse gas emissions. In this context, the development of sustainable renewable energy sources has become a strategic necessity. Among these sources, offshore wind energy has attracted considerable attention owing to its high power-generation potential, environmental sustainability, and alignment with global carbon-reduction goals.

Offshore wind turbines can generally be classified into fixed-bottom and floating systems based on their support structures. In water depths of less than approximately 50 m, fixed-bottom structures such as monopiles and jackets are typically considered economically viable. However, at greater water depths, floating wind turbines offer significant technical and economic advantages. Common configurations of floating support structures include barge, tension-leg platform, semi-submersible, and spar systems. Among these concepts, semi-submersible platforms have attracted particular interest because of their favorable stability characteristics, relatively low mooring-system costs, ease of transportation and installation, and the possibility of assembling the entire turbine at the port prior to deployment.

A semi-submersible floating wind turbine system consists of several main components, including blades, nacelle, hub, tower, floating platform, mooring lines, a heave plate, and connection elements such as fairleads (Fig. 1). These components are simultaneously subjected to aerodynamic loads, hydrodynamic forces, and control-system actions, resulting in a highly coupled dynamic behavior. Consequently, an accurate analysis of such systems requires a coupled aero–hydro–servo–elastic modeling framework.

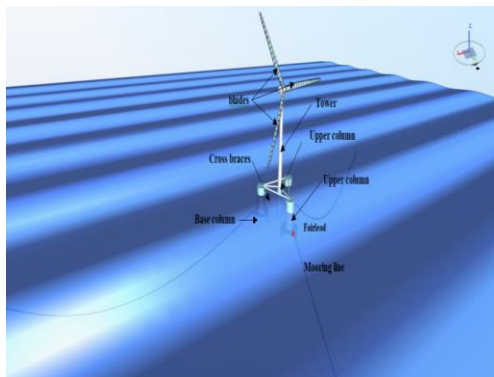


Figure 1. Components of FOWT

Early studies, such as Withee [1] and Wayman [2], demonstrated that platform motions can significantly influence the aerodynamic response and overall dynamic behavior of floating wind turbines. Matha et al. [3] further highlighted the importance of simultaneously considering aerodynamic, hydrodynamic, and mooring effects in the analysis of floating wind turbine systems. More recently, Yang et al. [4] showed that interactions between structural dynamics and the turbine control system can modify the frequency characteristics and vibration responses of the system. Despite these advances, the geometry of the floating platform has often been treated as fixed in many studies, and the influence of geometric variations on the overall dynamic behavior has been investigated less systematically.

On the other hand, several studies have examined hydrodynamic effects and nonlinear phenomena in the response of floating wind turbines. Xu et al. [5] investigated the influence of nonlinear wave loads on the motion responses of floating platforms, while Li and Bachynski [6] used CFD simulations to demonstrate that viscous effects may impose limitations on the application of hydrodynamic coefficients derived from linear potential-flow theory. Nevertheless, in many of these studies, the primary focus has been placed on hydrodynamic modeling or nonlinear effects, and the analyses have generally been conducted for a single predefined platform configuration.

From a design perspective, a number of studies have also explored the influence of structural and geometric characteristics on the performance of large offshore wind turbines Ferri et al. [7] Sandua Fernandez et al. [8] For instance, Ferri et al. investigated the influence of column spacing on the dynamic response of a semi-submersible platform supporting a 10 MW wind turbine using linear frequency-domain analysis. More recent studies have proposed alternative floating platform configurations aimed at improving dynamic performance. For example, He et al. [9] introduced a multi-column floating platform designed to support a 6 MW wind turbine and showed that variations in mass distribution and platform geometry can influence motion responses, particularly under severe environmental conditions. However, a systematic investigation of multiple geometric parameters affecting semi-submersible platform behavior within a framework that accounts for coupled aerodynamic, hydrodynamic, and control effects has not yet been comprehensively reported.

In the present study, the geometry of a semi-submersible platform is examined as a design variable within a coupled aero–hydro–servo–elastic modeling framework. The analysis focuses on the influence of several key geometric parameters, including the diameter of the offset columns, the radial distance of the columns from the platform center, the column height, and the geometric characteristics of the heave plate (diameter and thickness), on the six-degree-of-freedom motion responses and the frequency characteristics of the system within the dominant wave range. To this end, a two-stage analysis approach is adopted. First, linear frequency-domain analyses are performed to conduct a preliminary parametric screening. Subsequently, selected configurations are further evaluated through nonlinear time-domain simulations. The simulations are carried out using a coupled numerical tool developed for the analysis of floating wind turbine systems. This framework allows for a systematic assessment of the sensitivity of dynamic responses to geometric variations and may help provide further insight into the role of key design parameters in the performance of semi-submersible floating platforms.

2. Governing equations

The dynamic behavior of a floating wind turbine results from the simultaneous interaction of aerodynamic, hydrodynamic, hydrostatic, and mooring-induced forces and a wide range of environmental actions (Fig. 2).

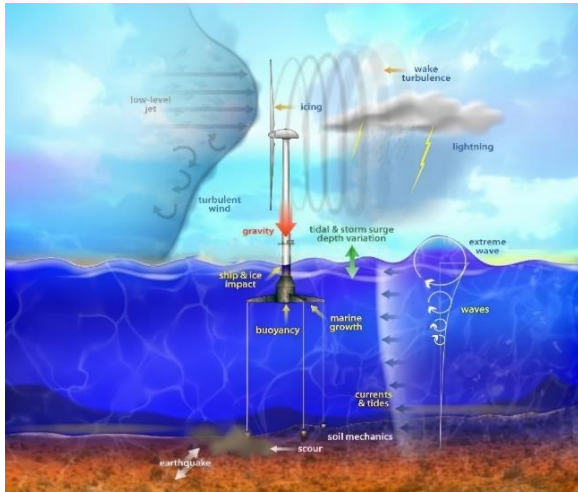


Figure 2. Forces acting on the FOWT [10]

Because environmental loads are inherently time-dependent and the interactions among different system components are largely nonlinear, time-domain analysis is required to realistically represent the system response.

Within this framework, the structural response is not determined solely by the magnitude of the applied loads but also by the distribution of mass, hydrostatic restoring characteristics, geometric properties governing fluid–structure interaction, and the coupling between the six degrees of freedom.

Time-domain simulations enable a detailed representation of transient dynamics, oscillation amplitudes, potential resonance phenomena, slow-drift motions, and the spectral characteristics of the response. Accordingly, the displacements, velocities, and accelerations of the system in the six degrees of freedom—surge, sway, heave, roll, pitch, and yaw—are calculated as time series. These time histories provide the basis for statistical analyses such as mean values, standard deviations, maximum responses, and power spectral densities, and therefore constitute an effective framework for comparing different floating platform configurations.

The general equation of motion governing the system can be expressed as

$$M\ddot{X} + C_v\dot{X} + f_{int} - f_{ext} = 0 \quad (1)$$

where X denotes the vector of generalized displacements, M is the structural mass matrix, and C_v represents the effective structural damping matrix. The vector f_{ext} includes environmental loads generated by wind, waves, and current, while f_{int} represents the internal and restoring forces associated with the structural configuration.

These internal forces arise from several physical mechanisms, including the distribution of mass within the system, the relative positions of the center of gravity and the center of buoyancy, hydrostatic restoring stiffness, rotational coupling associated with roll and pitch motions, nonlinear restoring effects of the mooring system, and instantaneous variations in the effective moment of inertia resulting from rotor–platform interaction. Consequently, f_{int} represents the combined restoring and equilibrium forces governed by the geometry, buoyancy, stability characteristics, and structural arrangement of the floating system.

When hydrodynamic forces associated with fluid–structure interaction are incorporated, the equation of motion can be written in the commonly used offshore hydrodynamic form

$$(M + M_a)\ddot{X} + B_d\dot{X} + CX = F(t) \quad (2)$$

where M_a is the added mass matrix, B_d represents the hydrodynamic damping matrix, C denotes the hydrostatic restoring matrix, and $F(t)$ is the vector of time-dependent environmental loads.

The coefficients M_a , B_d , and C depend on the hull geometry, the displacement pattern of the surrounding fluid, the mass distribution of the structure, and the buoyancy characteristics of the system. As a result, the dynamic response of the floating platform is governed not only by the intensity of environmental forcing but also by the manner in which these loads are reflected through the coefficients of the governing motion equation.

This dependence becomes particularly significant in vertical and rotational motions. Variations in the effective submerged area and the spatial arrangement of submerged components can increase added mass and hydrodynamic damping in the heave direction, thereby reducing heave response amplitudes. Because vertical and rotational modes are dynamically coupled, modifications in vertical hydrodynamic coefficients can also influence roll and pitch responses. Consequently, a considerable portion of the observed platform dynamics is directly associated with variations in hydrodynamic and hydrostatic coefficients induced by the structural configuration.

2.2 Aerodynamic Forces

Aerodynamic loads acting on wind-exposed structural components are calculated as

$$F_{aero} = \frac{1}{2}\rho V_P^2 C_D A \quad (3)$$

where ρ is the air density, V_P represents the wind velocity component normal to the structural member, C_D is the drag coefficient, and A is the projected area.

For the turbine blades, aerodynamic loads are computed using the Blade Element Momentum (BEM) method. In this approach, the aerodynamic force on each blade element is determined based on the relative wind velocity, the induced velocity field generated by the rotor, and the instantaneous rotational state of the blades. The extended BEM formulation presented by

Hansen [11,12] enables the simulation of unsteady aerodynamic conditions, including wind fluctuations, variations in rotor angular velocity, and turbulent flow effects. Consequently, aerodynamic forces are incorporated into the governing equations as time-dependent loads.

2.3 Hydrodynamic Forces

Floating structures typically exhibit responses within three characteristic frequency ranges: the wave-frequency range associated with primary wave excitation, the high-frequency range related to structural elastic modes, and the low-frequency range arising from wind-wave interaction and slow-drift phenomena. In time-domain simulations, these components appear simultaneously in the response, enabling the identification of dominant modes and the assessment of system stability.

For semi-submersible platforms, the natural periods of heave, roll, and pitch motions are typically greater than 20 s, while surge, sway, and yaw motions often exceed 100 s Massie et al. [13]

Hydrodynamic loads acting on slender structural members are evaluated using the Morison equation. [14]

$$F_{hydro}(z) = \rho C_D R |u - \dot{x}|(u - \dot{x}) + \pi \rho R^2 a + (C_M - 1)\pi \rho R^2 (a - \ddot{x}) \quad (4)$$

where R is the member radius, u and a denote the water particle velocity and acceleration, and x , \dot{x} , and \ddot{x} represent the displacement, velocity, and acceleration of the structural member.

For large-diameter members where the assumptions underlying Morison's equation are no longer valid, the inertia coefficient is corrected using the MacCamy-Fuchs formulation. [15]

$$C_M = 4\pi(kr)^2 \sqrt{A_1(kr)} \quad (5)$$

which plays an important role in the hydrodynamic modeling of semi-submersible columns.

2.4 Numerical Damping

To prevent nonphysical oscillations in the numerical solution, the Hilber-Hughes-Taylor (HHT) time integration scheme is employed. This method represents an extension of the Newmark- β formulation and

introduces controlled numerical damping at high frequencies while preserving the accuracy of the physical response.[16]

2.5 Mooring System

The mooring system was modeled using a static catenary formulation. In this formulation, the catenary shape parameter s_d is obtained by solving the nonlinear equilibrium equation

$$2x \sinh\left(\frac{s_d d}{2}\right) - \sqrt{L^2 - h^2} = 0 \tag{6}$$

where d and h are the horizontal and vertical distances between the two end nodes, respectively, and L is the unstretched line length. The horizontal coordinate of the left node is then computed as

$$x_{\text{left}} = \frac{1}{2}(l_{nl} + d_l - d_s - d) \tag{7}$$

These nonlinear equations are solved using the Newton–Raphson iterative method. The resulting equilibrium configuration is used to determine the mooring restoring characteristics and their contribution to the coupled dynamic response of the platform.

3. Numerical simulation

To investigate the dynamic behavior of the floating offshore wind turbine (FOWT), numerical simulations were carried out using the Aero-Servo-Hydro-Elastic Simulation (ASHES) software. [17] This platform integrates aerodynamic, hydrodynamic, structural, and turbine control models, enabling a comprehensive evaluation of the coupled system response under combined wind and irregular wave loading (Fig. 3).

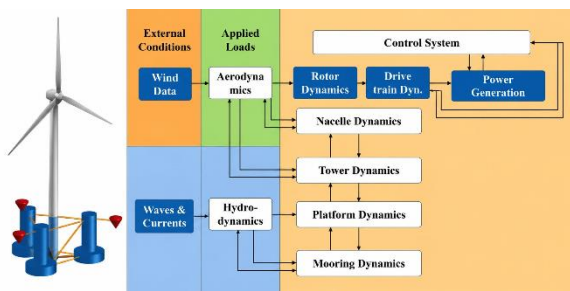


Figure 3. Algorithm of the simulation

The adopted methodology follows a multi-stage numerical framework designed to systematically explore the design space of the semi-submersible platform and to identify configurations suitable for more detailed dynamic analyses. First, environmental data corresponding to the study region were collected and implemented as simulation inputs. These data include both statistical descriptors of the environmental conditions and the associated time histories of environmental loading.

Subsequently, the numerical model was validated against a well-established reference platform to assess the accuracy of the aero-hydrodynamic coupling, the performance of the turbine control system, and the capability of the model to reproduce realistic time-domain responses. After the validation stage, linear parametric analyses were conducted to identify appropriate design ranges and to evaluate the sensitivity of structural responses to key geometric parameters. In addition to frequency-domain indicators, selected transient characteristics in the time domain were also considered during the evaluation process.

After narrowing the design space, nonlinear models were developed to investigate geometric effects, multi-physics coupling mechanisms, and the structural response under more realistic environmental loading conditions. At this stage, time-domain simulations played a critical role in identifying transient behaviors, capturing nonlinear effects, and providing a more realistic assessment of the performance of the investigated configurations.

Finally, the combined outcomes of linear and nonlinear analyses, together with the evaluation of time-domain responses, provided the basis for selecting suitable configurations for advanced dynamic investigations. The remainder of this section presents the environmental data, describes the platform development and screening procedure, and evaluates the selected models within a refined numerical framework.

3.1. Environmental Conditions

Data The environmental conditions used in the simulations were defined based on oceanographic and meteorological data corresponding to an offshore region located approximately 17 km from the coast of Jask, Iran (Fig. 4).

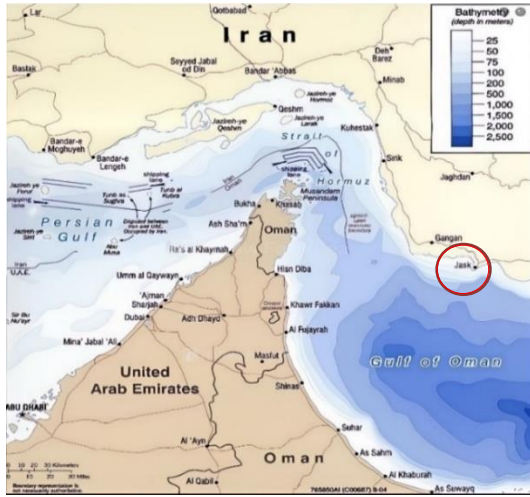


Figure 4. Area under study [18]

To ensure a realistic representation of the site characteristics, the required datasets were compiled from several reliable sources, including the GEBCO [19] global bathymetric database, the National Cartographic Center of Iran, and the NCC Tide software. [20]

Based on these datasets, a set of key environmental parameters was selected to define the boundary conditions and environmental loading in the numerical simulations. These parameters represent typical operational conditions in the study area and were implemented within the coupled simulation framework to reproduce realistic environmental forcing. The resulting environmental parameters used in the simulations are summarized in Table 1 Oceans.[21]

Table 1. Environmental load

Item	Value
Wind	10.5 [m/s]
Wave	5 [m]
Tide	3.5 [m]
Current	0.78 [m/s]
Bathymetry	200 [m]

These environmental conditions were used to generate loading scenarios in the coupled aero-hydrodynamic simulations and provided the basis for evaluating the dynamic response of the floating system under realistic site conditions.

3.2. Numerical Model Validation

To evaluate the reliability of the developed numerical framework, a validation study was conducted using the OC4 DeepCwind semi-submersible platform supporting the NREL 5 MW reference wind turbine. [22] The geometric configuration, hydrostatic characteristics, and mass properties were reconstructed based on the official NREL documentation and the implementation reported by Ferri et al, ensuring full consistency with the OC4 benchmark definition. The principal properties of the platform are summarized in Table 1.

Table 2. 5MW NREL DeepCwind platform

5MW NREL DeepCwind platform	Value
Depth of platform base below SWL	20 [m]
Elevation of main column above SWL	10 [m]
Elevation of offset column above SWL	12 [m]
Length of upper column	26 [m]
Length of heave plate	6 [m]
Depth to top base column below SWL	14 [m]
Diameter of main columns	6.5 [m]
Diameter of offset columns	12 [m]
Diameter of heave plate	24 [m]
Diameter of pontoon and cross-braces	1.6 [m]
Platform CM location below SWL	13.5 [m]
Water depth	200 [m]

The OC4 DeepCwind platform constitutes a widely recognized benchmark for floating offshore wind turbine (FOWT) research, making it an appropriate reference for hydrodynamic validation. Moreover, Ferri et al, adopted herein as the primary comparison source, previously validated its numerical model against established OC4 reference datasets, including power spectral densities (PSD), response amplitude operators (RAOs), peak motion frequencies, hydrostatic parameters, and other benchmark quantities. The PSD results reported by Ferri are presented in Figure 5.

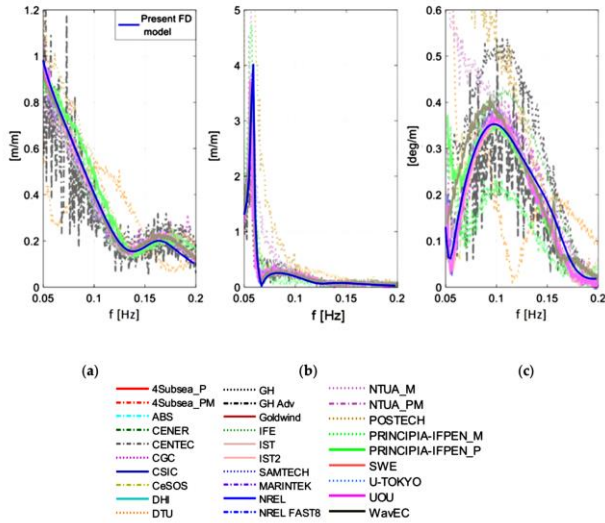


Figure 5. Comparison of the Response Amplitude Operators (RAOs) for the NREL 5-MW semisubmersible platform in (a) surge, (b) pitch, and heave Ferri, et al. [7,10]

A band-limited white-noise wave excitation within the frequency range of 0.05–0.25 Hz was applied in the surge direction to characterize the frequency-domain response of the system. The resulting PSDs of surge, heave, and pitch motions were extracted and compared against the reference data.

The comparison demonstrates strong agreement across all three degrees of freedom. In surge, both the dominant spectral peak and the overall energy distribution are accurately reproduced. In heave, the peak frequency and spectral shape closely follow the benchmark results, indicating consistent representation of radiation and restoring effects. Similarly, in pitch, the alignment of resonance frequency and peak magnitude confirms that the global hydrostatic and hydrodynamic stiffness characteristics are properly captured. The corresponding comparison between the present model and the reference results is shown in Figure 6.

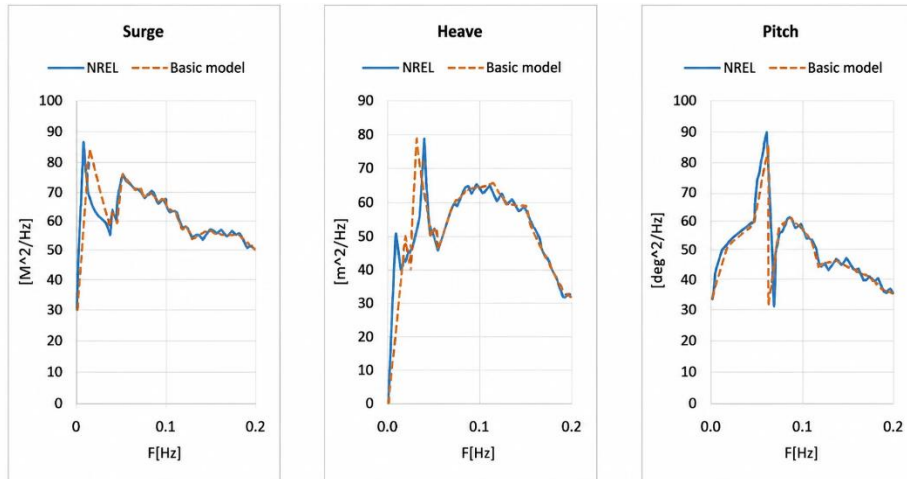


Figure 6. Validating the 5 MW model

For quantitative assessment, the RAOs of surge, heave, and pitch were evaluated against the OC4 reference values. The obtained RAOs are 0.84 and 0.81 in surge, 0.93 and 0.90 in heave, and 1.05 and 1.00 in pitch for the present and reference models, respectively, corresponding to relative deviations of 3.7%, 3.3%, and 5.0%. These discrepancies fall within the acceptable tolerance range typically reported for floating offshore structure simulations.

The minor differences can be attributed to modeling assumptions, including the equivalent linear stiffness representation of the mooring system, limited availability of viscous damping coefficients in the

reference dataset, and slight numerical variations in the treatment of low-frequency aerodynamic–hydrodynamic coupling. Nevertheless, the close agreement in spectral trends, resonance frequencies, and response amplitudes confirms that the developed numerical framework reliably reproduces the dynamic behavior of the OC4 DeepCwind platform.

Accordingly, the validated model is adopted as the baseline numerical framework for the subsequent parametric investigations and time-domain analyses.

3.3 Linear Parametric Analysis

Following the validation stage, an extensive design space consisting of 32 platform configurations was generated by varying the principal geometric parameters of the platform. The objective of this parametric investigation was to systematically examine the influence of heave-plate diameter, radial spacing of the offset columns, column diameter, and ballast height on the hydrodynamic characteristics of the platform, particularly the variations in added mass, hydrodynamic damping, and hydrostatic restoring stiffness within the framework of linear potential-flow theory.

The dynamic behavior of these 32 configurations was evaluated in the six degrees of freedom—surge, sway, heave, roll, pitch, and yaw—and subsequently compared with the reference platforms NREL 5-MW and DTU/Ferri 10-MW within a staged screening procedure.

This screening process resulted in the selection of 19 refined models that exhibited more stable hydrodynamic behavior and better consistency with accepted design criteria. The principal characteristics of these configurations are summarized in Table 3, while their response characteristics are illustrated in Figure 7.

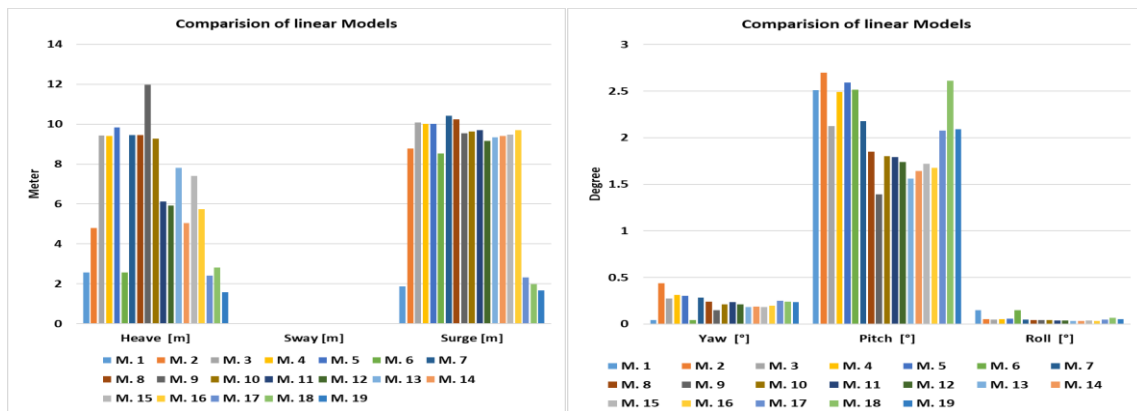


Figure 7. Data for the six degrees of freedom motions of the linear models

Table 3. Finalized components of the linear models

Model number	Height of ballast	Offset column diameter	Offset column distance	Heave plate diameter
5MW NREL	30	12	28.87	24
DTU 10 MW	28.30	16.97	31	33.94
3	28.30	16.97	37	33.94
4	25	16.97	37	33.94
5	27	16.97	37	33.94
6	26	16.97	38	31
7	26	17	38	31
8	28	17	39	31
9	28	17	41	31
10	29.5	16	41	29
11	29	16	40	22
12	28	16	31	22
13	28	17	41	25
14	29	17	41	20
15	32	16	41	23
16	30	16	41	21
17	28	15	39	20
18	30	13	41	23
19	27.6	12	41	21

Although linear analysis provides valuable insight into the fundamental response characteristics of the platform, the observed behavior in several configurations—particularly those featuring larger heave plates or thicker columns—suggested that viscous damping variability, motion-dependent buoyancy, and aero-hydrodynamic coupling may play a more significant role than can be fully captured by the linear model. These observations indicated the necessity of extending the analysis toward a nonlinear modeling framework.

Among the 19 refined configurations, Configuration 19 demonstrated the most balanced combination of added mass, effective damping, and restoring inertia, while also showing the closest agreement with the reference datasets. Consequently, this configuration was selected as the baseline model for nonlinear analysis.

3.3. Nonlinear model

To overcome the limitations of the linear formulation and to reproduce more realistic system behavior under operational sea states, Configuration 19 was

reconstructed within the ASHES environment with the activation of the principal nonlinear physical mechanisms.

The environmental and structural parameters used for the reconstruction of Configuration 19 within the ASHES simulation environment are summarized in Table 4.

Table 4. Simulation data for environmental forces and turbine components

Atmosphere	Unit
Air temperature	15 c°
Wind speed	10.5 m/s
Wind angle	Front
Shear profile	On
Sea state	unit
Mean sea level	0
Tidal level	3.5 m
Waves type	Irregular
Waves height	5 m
Waves period	10.5 s
Waves angle	Front
Waves spectrum type	Joint North Sea Wave Project (JONSWAP)
Simulation scheme	Equal frequency
Number of extremes duration	10 600 s
Time step	1 s
Time buffer	15 s
Sea bed	200 m
Wind turbine	Unit
Rotor type	DTU-10MW
Rotor length	86.366 m
Rotor mass	42781.6 Kg
Main shaft length	10 m
Main shaft radius	0.8 m
Nacelle frame mass	240000 Kg
Nacelle frame CM horizontal	-1.9 m
Nacelle frame CM vertical	1.75 m
Support structure	Unit
Semisubmersible draft	19.86 m
Semisubmersible height	30 m
Semisubmersible main column diameter	8.2 m
Semisubmersible main column thickness	0.03 m
Semisubmersible offset column number	3
Semisubmersible offset column distance	41
Semisubmersible offset column upper diameter	12 m
Semisubmersible offset column heave plate height	20% height
Semisubmersible offset column heave plate diameter	21 m

Semisubmersible offset column heave plate base thickness	0.06 m
Pontoons and cross section diameter	1.6 m
Pontoons and cross section thickness	0.04
Tubular tower top diameter	4.98 m
Tubular tower top thickness	0.019 m
Tubular tower base diameter	8 m
Tubular tower base thickness	0.027 m
Mooring line	Unit
Mooring line equivalent horizontal stiffness	150,000 N/M
Mooring line equivalent vertical stiffness	0 N/M
Mooring line diameter	0.0766 m
Mooring line anchor distance	1,000 m
Mooring line anchor depth	200 m
Mooring line fairlead center distance	12 m
Fairlead line distance	50 m
Mooring line number of elements	50
Mooring line distributed mass	130 Kg/m
Mooring line elastic modulus	18975E+11 Pa

At the initial stage of nonlinear model development, several key characteristics of the semi-submersible platform dynamics were identified as dominant contributors to nonlinear behavior. These include motion-dependent buoyancy, viscous drag variability, aero-hydrodynamic coupling, and the influence of the heave plate on added mass coefficients. The structure of the nonlinear model was therefore designed to explicitly capture these effects.

Second-order viscous drag was implemented by replacing the linear drag formulation with a quadratic expression based on the relative velocity between the structure and the surrounding fluid. The viscous drag coefficients associated with the heave plate were directly calibrated using viscous hydrodynamic analyses.

Nonlinear hydrostatic restoring forces were introduced by computing hydrostatic stiffness based on the instantaneous submerged volume and the evolving wetted surface geometry rather than using a constant stiffness matrix. This feature is particularly important

for the heave plate and offset columns, whose buoyancy contributions vary with platform motion.

The fully coupled aero–hydro–servo–elastic framework was also activated, allowing the rotor dynamics, turbine controller, tower flexibility, and platform motion to interact simultaneously. This integrated approach ensures that the wind–wave–structure interaction is represented without artificial decoupling.

For the heave plate, the linear potential flow coefficients of added mass and hydrodynamic damping were replaced with coefficients derived from viscous hydrodynamic analysis. This modification improves the realism of the predicted heave and pitch responses, where the hydrodynamic influence of the heave plate is particularly significant.

To maintain computational efficiency, several secondary effects were simplified. Higher-order wave forces and nonlinear wave run-up were not explicitly modeled, the platform structure was assumed to behave as a rigid body, and the incoming wave field was represented using linear potential flow theory. These simplifications reduce computational complexity while preserving the dominant nonlinear mechanisms governing the platform dynamics.

Figure 8 shows the schematic layout of the semi-submersible floating wind turbine used for the nonlinear

configuration study. The main structural elements, including the tower, upper and base columns, heave plates, cross braces, and mooring lines, are indicated.

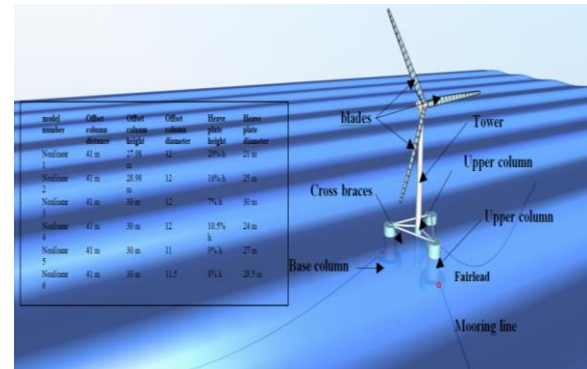


Figure 8. The image on the left is related to the components of the simulated nonlinear models, while that on the right is related to the simulation environment of the software

To systematically evaluate nonlinear structural behavior, six additional nonlinear models were developed based on the baseline configuration (Configuration 19). These models incorporate targeted geometric variations in the diameter and thickness of the heave plate, the diameter and height of the offset columns, and the radial spacing between the columns. The detailed geometric parameters of these configurations are summarized in Table 5.

Table 5. Finalized components of nonlinear models

Model number	Offset distance	Offset column height	Offset column diameter	Heave plate height	Heave plate diameter [m]
Nonlinear 1	41 m	27.68 m	12	20% h	21 m
Nonlinear 2	41 m	28.98 m	13	16% h	25 m
Nonlinear 3	41 m	30 m	12	7% h	30 m
Nonlinear 4	41 m	30 m	10	10.5% h	24 m
Nonlinear 5	41 m	30 m	11	9% h	27 m
Nonlinear 6	41 m	30 m	11.5	8% h	28.5 m

In the final stage of the simulations, the nonlinear models were coupled with a complete environmental field including both wind and wave forcing. Aerodynamic and hydrodynamic loads were directly applied in time-domain simulations, and the incoming wave field was defined as a combination of the local irregular wave spectrum and a long-period swell component. This representation preserves the simultaneous contribution of short-period and long-period excitations, which is particularly important for accurately capturing heave and pitch responses.

By maintaining the total platform mass constant at 14,710 tons, the responses of the six nonlinear configurations were evaluated and compared with the OC4 reference platform. The comparison of the Response Amplitude Operators (RAOs) in surge, heave, and pitch indicates that all investigated configurations exhibit stable dynamic behavior and remain within the expected response range of semi-submersible floating structures.

Therefore, the developed modeling framework demonstrates adequate capability in representing hydrodynamic response and wind–wave–structure interaction, providing a reliable basis for the analysis and interpretation of the simulation results presented in the following section.

4. Results

In order to compare the motion-response limits and identify the best-performing configuration, simulations were conducted for the 10 MW nonlinear models and the NREL 5 MW turbine. Fig. 9 compares the NREL 5 MW simulation results with those of the 10 MW nonlinear models. As shown, Models 3 and 6 exhibit the best performance among the considered cases. It is also noteworthy that nonlinear Model 1 is regarded as an upgraded version of linear Model 19, which was used as the basis for the nonlinear design.

To establish an appropriate and standard motion-response benchmark, the results were further compared with those of a 5 MW wind turbine, which has a smaller overall system in terms of the turbine structure, floating platform, mooring lines, tower, and blades. The final analysis was then conducted to discuss the contributions of the driving and resisting forces associated with the platform, tower, turbine, and mooring lines. The results are presented in terms of translational and rotational motions (surge, pitch, and heave) and discussed across the corresponding figures.

Heave and pitch responses were used to assess the dynamic response of the system. For surge, the influence of the mooring lines was significant, and the associated response-frequency range (0.004–0.038 Hz) was therefore considered only partially representative of the turbine motion. Accordingly, heave and pitch motions were adopted as the primary indices of turbine motion.

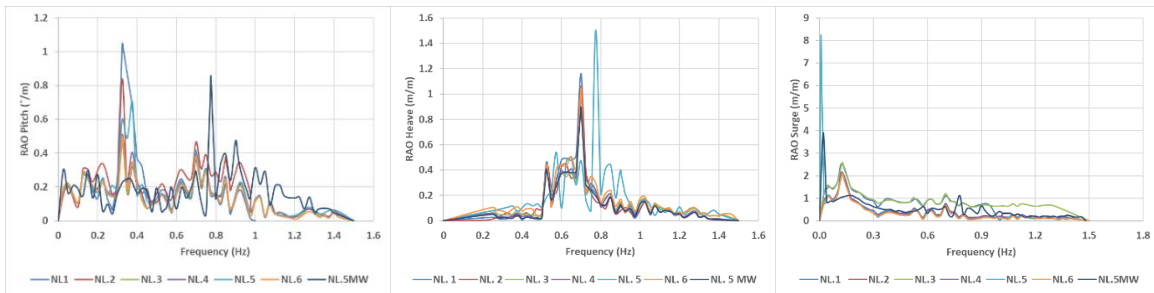


Figure 9. Comparing the results of non-linear models 1 to 6 with the NREL 5MW

4.1. Comparing nonlinear models

The response spectra of five nonlinear models were evaluated for heave and pitch motions. The variations among these models were based on the waterplane area, the offset-column spacing to improve stability against rotor-induced motions, and the heave-plate design to reduce vertical motion in the z-direction by lowering the natural frequency. To control and minimize heave motion, the study focused on optimizing the diameter and thickness of the heave plate.

Model 6, with a heave-plate diameter of 28.5 m and a height equal to 8% of the base height, showed the best performance among the considered structures. Model 3, with an offset-column diameter of 12 m and a heave-plate diameter of 30 m, exhibited performance closest to that of Model 6. Model 5 showed poor performance because of the disproportionate height of the heave plate, which was only 9% of the offset-

column height, despite having an offset-column diameter of 11 m and a heave-plate diameter of 27 m. It is worth noting that the limited influence of heave-plate thickness was also reported by Ferri et al, whereas the effects of the plate height relative to the offset-column height, as well as their proportional relationship, are clearly evident here. Model 2, with a heave-plate diameter of 25 m and an offset-column height of 28.98 m, exhibited weaker performance than Model 6. Model 1, with a heave-plate diameter of 21 m and a height of 27.98 m, did not perform satisfactorily. Therefore, a heave plate with smaller thickness and larger diameter provides acceptable results within a certain range, provided that the offset-column heights are similar.

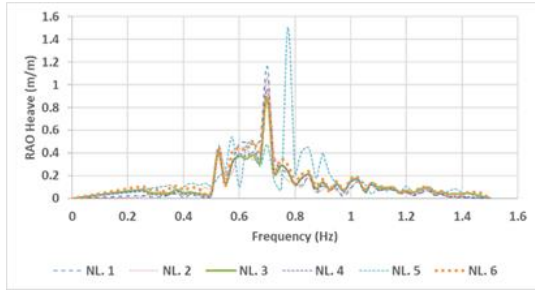


Figure 10. Comparing the results of model 6 with other nonlinear ones in Heave motion

Overall, two criteria were considered to reduce and balance the structural motions. First, the diameter of the offset columns was selected to minimize platform motions by reducing the drag force. Second, the distance of the offset columns from the center of the platform was adjusted to improve the platform balance against environmental loads and rotor-induced motions by increasing the structural inertia. Based on these considerations, the offset columns were placed at a distance of 41 m from the center of the platform. The following results were obtained by varying the offset-column diameter. Figs. 1 and 2, corresponding to nonlinear Models 1 and 2, showed weaker performance than Models 3 and 6, which have smaller offset-column diameters, thereby confirming

the observations discussed earlier. The results for Models 3 and 6 are then discussed in detail, considering the main design parameters of interest.

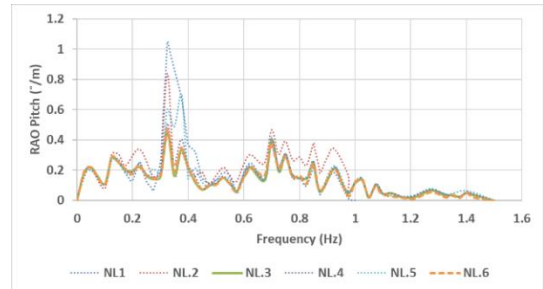


Figure 11. Comparing the results of model 6 with other nonlinear ones in pitch motion

4.1.1. Effects of diameter and thickness of heave plate

In FOWTs and floating offshore platforms, the platform motion in the heave direction is primarily governed by the damping and added mass induced by the heave plate. Furthermore, the heave plate significantly influences angular motions, such as pitch, through its contributions to the hydrodynamic added mass and damping. The present study investigates the influence of the heave plate on vertical platform motions (Fig. 12).

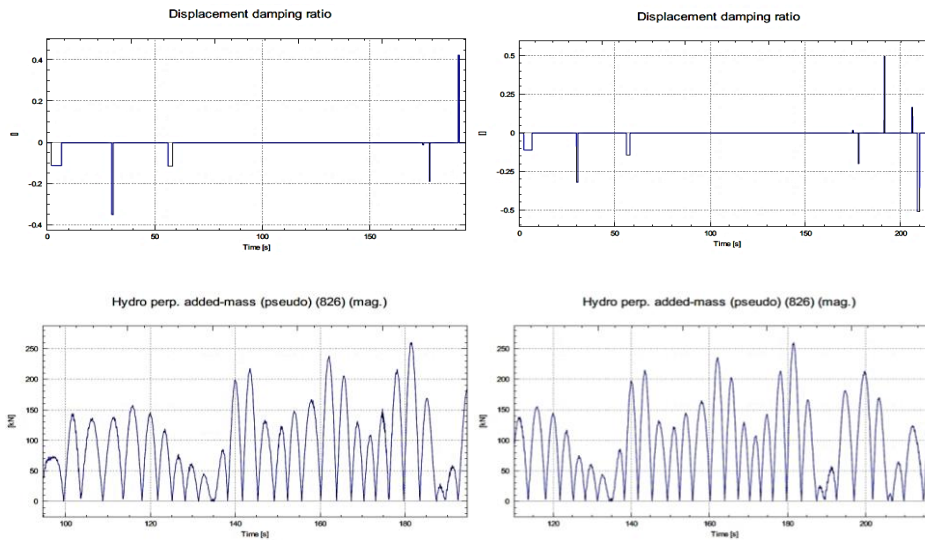


Figure 12. Results related to added mass and damping for model number 3 in the left column and model number 6 in the right column

As shown in Fig. 12, the damping values for Model 6 are 0.1 units higher than those for Model 3. In addition, Model 6 exhibits an added mass approximately 10 units

higher than that of Model 3, despite having a smaller diameter and greater thickness. These findings indicate that the geometric configuration of the heave plate,

particularly the interplay between diameter and thickness, plays a significant role in the hydrodynamic response of the system.

4.1.2. Effects of Offset-Column Diameter and Spacing

In a semi-submersible FOWT platform, reducing the offset-column diameter and selecting an appropriate inter-column spacing can decrease the viscous drag force and shift the hydrodynamic loading toward a more inertia-dominated response, which can improve the

pitch and yaw behavior of the turbine. A smaller offset-column diameter reduces the projected area and, therefore, the viscous drag contribution. Moreover, geometric modifications of the offset columns and their spacing alter the added-mass-related (inertial) component of the hydrodynamic loading and can lead to a favorable change in the pitch response. Consequently, a configuration with smaller offset columns and optimized spacing can reduce the drag contribution while maintaining (or enhancing) the inertial component, resulting in improved controllability and overall performance of the floating wind turbine (Fig. 13).

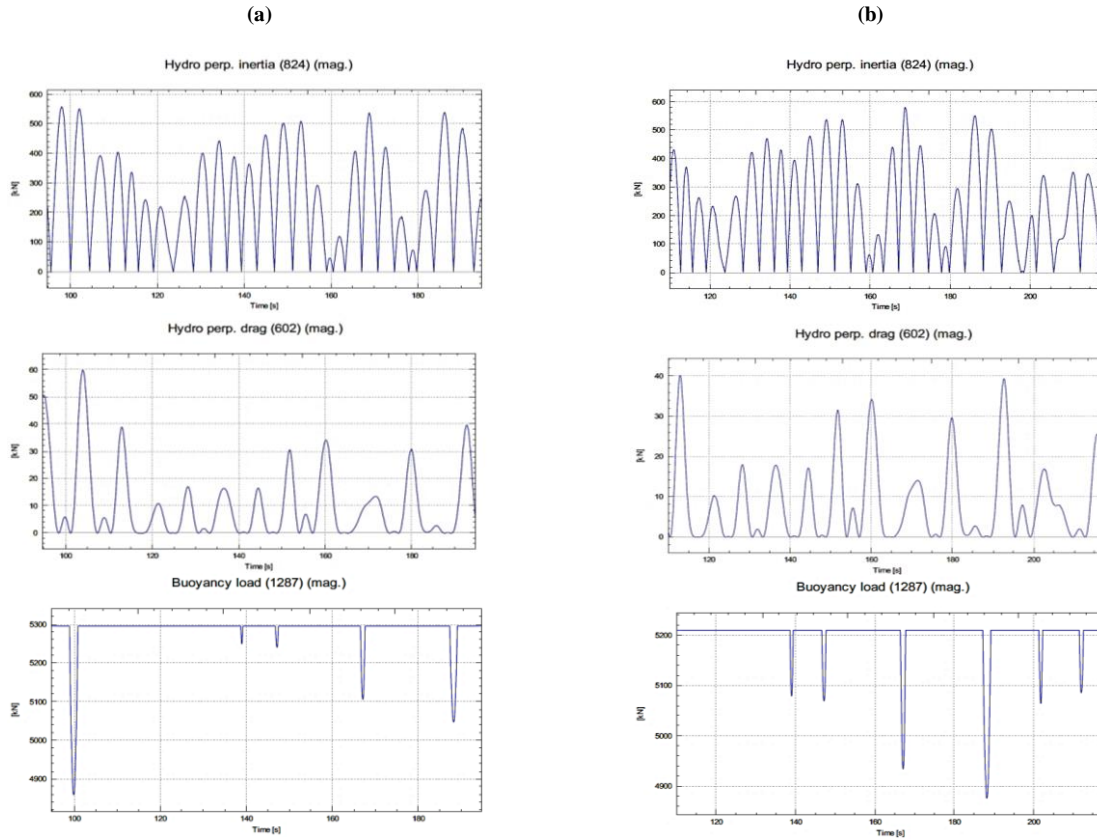


Figure 13. Results related to drag, inertia, and buoyancy load for model number 3 in the (a) Section and model number 6 in the (b) section

As shown in Fig. 13, Model 3 exhibits a peak drag force of approximately 60 kN and an inertial force of about 560 kN, whereas Model 6 shows corresponding values of approximately 40 kN and 580 kN, respectively. This trend is consistent with the comparative frequency-response spectra between Models 3 and 6. It is also noteworthy that the buoyancy force remains essentially constant across all models because the global buoyancy characteristics were kept consistent based on the adopted design dimensions. Therefore, the differences observed in Fig. 13 primarily reflect the effects of the offset-column geometric modifications on the hydrodynamic force components.

4.2. Effects of natural frequency on the structure

Vibrations induced by environmental loads are among the main challenges in the design and operation of offshore structures, particularly in deep-water applications. Consequently, accurate design—especially with respect to dynamic behavior and vibration performance—has become increasingly critical, even with the use of large-scale structural components. For floating platforms, resonance may occur in the heave and pitch degrees of freedom due to nonlinear wave–structure interaction effects. Moreover, sea states are inherently irregular and contain multi-frequency energy content. Although the first-order wave components typically have the largest amplitudes, higher-frequency excitations with smaller magnitudes may still influence the structural response and can be amplified by second-order effects, Chakrabarti, et al. [23] This mechanism can introduce excitation components with frequencies close to the platform natural frequencies, thereby increasing the likelihood of resonance. Therefore, in this study, the platform dimensions were selected to shift the natural frequencies away from dominant wave-energy regions by increasing the effective stiffness and to reduce the adverse effects of environmental loads. Figure 14 presents the dynamic responses of Model 6 and its corresponding natural frequency, which is relatively low and located within a favorable region of the response amplitude operator (RAO).

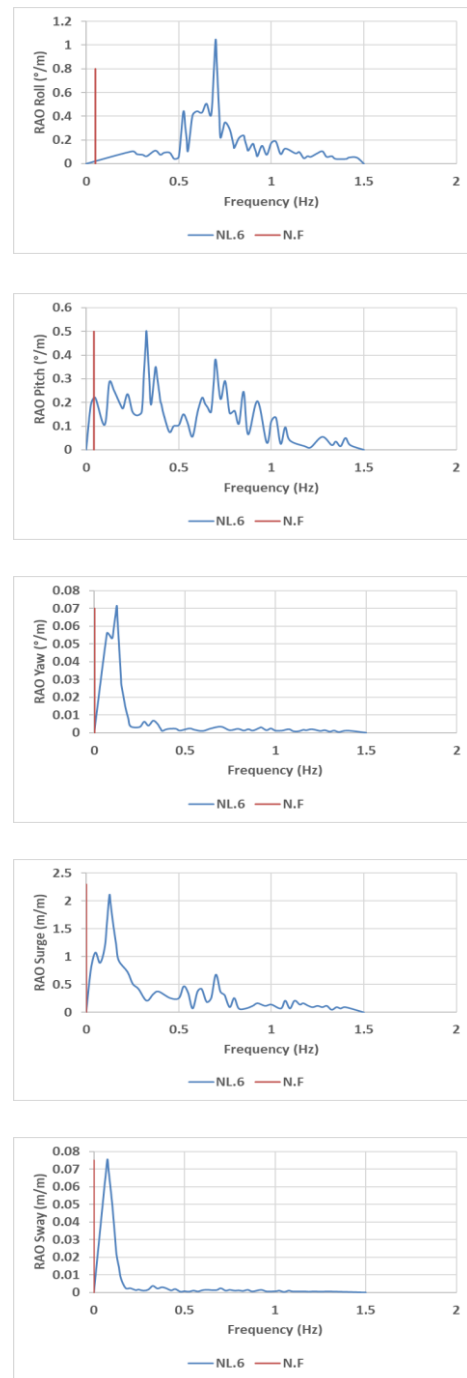
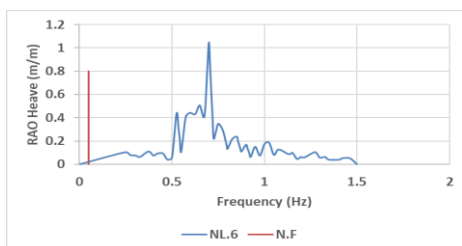


Figure 14. Position of natural frequency and dynamic motion frequency in finalized mode

4.3. Linear vs. nonlinear analysis of Model 6

Figure 15 compares the predicted motions of Model 6 obtained from linear and nonlinear simulations. The linear model yields noticeably larger motion amplitudes than the nonlinear model.



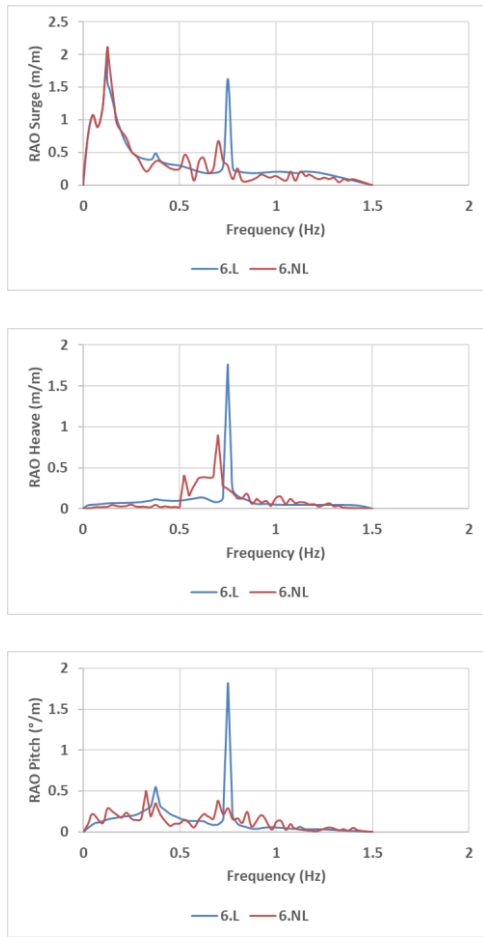


Figure 15. Comparative results of linear and nonlinear models

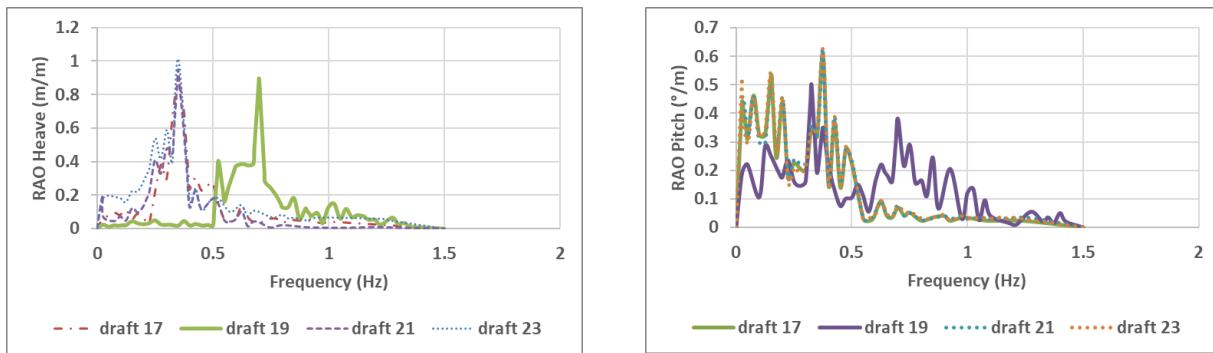


Figure 16. Comparative results of different draft depth in model 6

The results indicate that a 19-m draft provides the most favorable performance in pitch motion, whereas the heave response shows no substantial variation across the cases. It is important to note that these results were obtained for a platform height of 30 m, a wave height of 5 m, and a tide level of 3.5 m. Since changes in the offset-column height can significantly alter these outcomes, identifying the optimal draft for the current configuration was the primary objective of this analysis.

While linearization can provide reasonable estimates for small-amplitude responses, it may not adequately capture important nonlinear contributions to the excitation and damping, particularly when the relative motion between the platform and the free surface becomes large (e.g., near resonance or under long-period wave components). In such conditions, nonlinear effects associated with viscous drag and second-order wave loads can become significant, and linear models tend to overpredict motions due to simplified force representation and damping. Therefore, relying solely on linear predictions in similar sea states may lead to overly conservative response estimates and, consequently, uneconomical design margins.

4.4. Effect of the draft on model 6 results

The draft is a critical parameter influencing the motions of floating structures. Increasing the draft can significantly enhance the stability of a platform by increasing the submerged volume and, consequently, the restoring moments against environmental loads. In this study, four different draft configurations were investigated for Model 6—while maintaining constant geometric and environmental conditions—to assess their impact on the structure’s nonlinear behavior (Fig. 16).

4.5. Dynamic behavior of the platform in two operational and parked modes

This section investigates the impact of rotor operational states—Power Production versus Parked—on the platform’s dynamic responses. In the operational mode, a steady wind speed of 10.5 m/s (rated speed for the DTU 10 MW turbine) is applied at the hub height, representing the condition of peak aerodynamic thrust. The Response Amplitude Operators (RAOs) for surge, heave, and pitch are illustrated in Fig. 17, where red and blue curves distinguish the parked and operational states, respectively.

As depicted in Fig. 17, while all degrees of freedom (DOFs) exhibit distinct resonance peaks, a significant disparity is observed primarily in the pitch mode. In the operational state, the pitch RAO undergoes substantial attenuation compared to the parked condition. This phenomenon is attributed to the Aerodynamic Damping generated by the rotor’s thrust-velocity feedback loop. As the platform pitches, the relative wind speed at the hub changes, inducing fluctuations in the thrust force that act as a restorative, dissipative mechanism (anti-phase to the motion velocity).

This is because these DOFs are hydrodynamically dominated, where the restoration and damping are governed by hydrostatic stiffness and viscous/radiation damping of the submerged hull. In these modes, the contribution of aerodynamic forces to the total energy dissipation is negligible compared to the massive hydrodynamic added mass and damping of the semi-submersible platform. Consequently, the coupling between aerodynamic thrust and translational motions (surge/heave) is not strong enough to significantly alter the spectral response under the investigated conditions.

Conversely, the responses in surge and heave remain relatively insensitive to the rotor’s operational state.

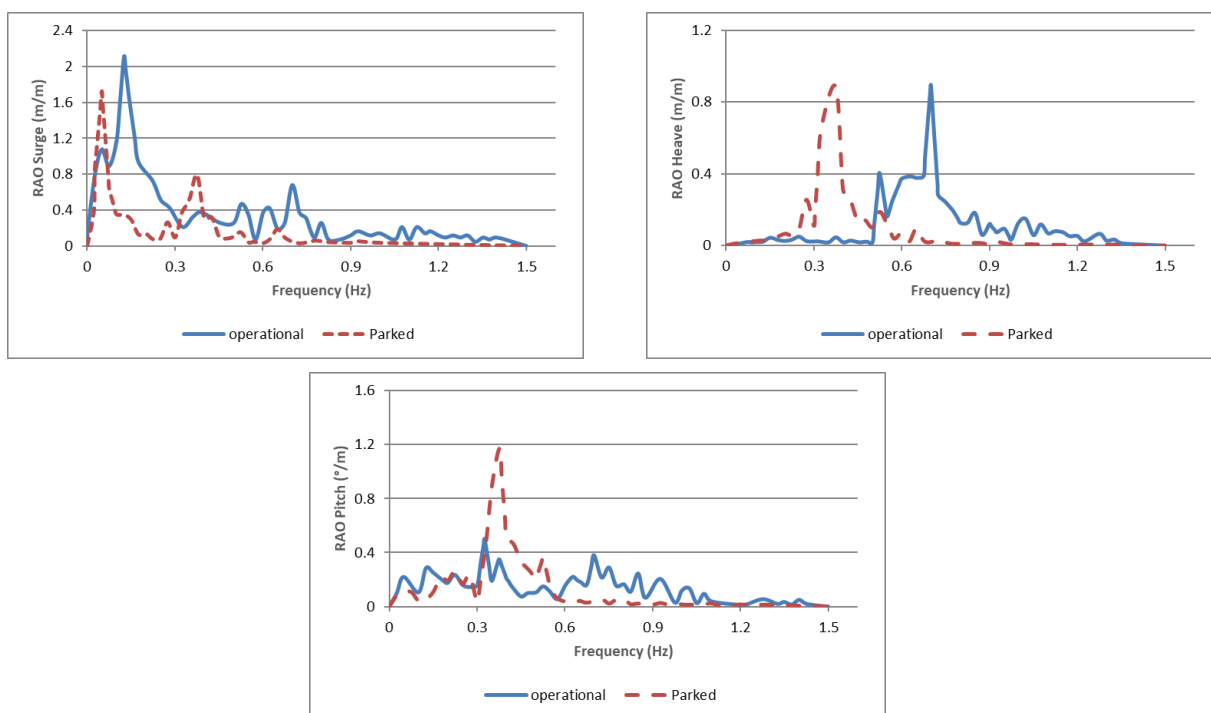


Figure 17. Finalized model in operational and parked mod

5. Discussion and Conclusions

This study aims to provide a deeper understanding of how geometric parameters and structural characteristics influence the dynamic behavior of semi-submersible platforms supporting floating wind turbines. The primary objective is to identify response trends within a prescribed design space. Accordingly, rather than seeking a single globally optimal configuration, the work adopts a parametric perspective to quantify the sensitivity of the platform’s dynamic responses to geometric/structural variations and to delineate design regions associated with more stable behavior.

To this end, the analyses were performed in two stages. First, linear simulations were used for rapid screening of candidate geometries and for identifying overall response tendencies. Subsequently, nonlinear time-domain simulations were carried out to obtain a more realistic assessment of system behavior. Time-domain analysis enables direct evaluation of response time histories, more accurate estimation of motion amplitudes, and a detailed examination of coupling among degrees of freedom—features that are not fully captured by purely linear approaches. Comparison of the two approaches further suggests that, while linear analysis is effective for preliminary trend identification, it may overpredict the dynamic response for certain configurations; therefore, nonlinear time-domain simulation is

required for more reliable performance assessment.

The results indicate that the heave-plate geometry—particularly its diameter and thickness—has a pronounced effect on the dominant platform responses. The discussion therefore focuses on the three primary degrees of freedom, i.e., surge, heave, and pitch, which govern the dynamic behavior of semi-submersible platforms. The remaining degrees of freedom (sway, roll, and yaw) exhibit comparatively small amplitudes and negligible contributions to the overall response in the present cases and are thus not examined in detail.

The results further show that changes in heave-plate geometry can effectively modify the platform response through their influence on added mass and hydrodynamic damping. Within the investigated parameter range, heave-plate diameters of approximately 24–30 m and thicknesses of about 7–10.5% of the offset-column height yield more stable responses with reduced motion amplitudes. This finding is important because it indicates that the heave-plate parameters, although local geometric features, affect the coupled dynamics of the entire system through changes in the hydrodynamic coefficients. Within this range, the increase in hydrodynamic damping improves performance without inducing unfavorable resonance near the dominant wave-frequency content.

Nevertheless, the platform dynamics cannot be attributed solely to the heave-plate geometry. Other geometric and structural parameters—including the diameter and height of the offset columns, inter-column spacing, waterplane area, structural mass distribution, and mooring-system characteristics—also play an important role in shaping the overall response. Time-domain simulations indicate that these parameters can alter the response patterns through coupling between translational and rotational motions. Hence, a key outcome of this study is that platform performance should not be assessed based on a single parameter in isolation; instead, the combined effects of multiple geometric and structural variables should be evaluated within an integrated parametric framework.

Among the examined configurations, a heave-plate diameter of approximately 28.5 m and a thickness of about 8% of the offset-column height produce a more balanced response relative to the other cases. In this configuration, the time-domain motion amplitudes in the dominant degrees of freedom are reduced, and the oscillation energy is more evenly distributed among the motion modes. Notably, several nearby configurations exhibit comparable performance. Therefore, the present results support the existence of a favorable design range rather than a unique optimal geometry. This insight is especially relevant at the conceptual-design stage, where targeting a stable and acceptable design region may be more robust than relying on a single optimum.

Overall, the main contribution of this work is the combined use of rapid linear screening and nonlinear time-domain evaluation to systematically investigate the concurrent influence of key geometric parameters on the coupled surge, heave, and pitch responses. Compared with studies that rely primarily on linear analysis or vary a single parameter, the present work demonstrates how simultaneous changes in heave-plate geometry and platform structural arrangement can modify the global dynamic behavior through their effect on hydrodynamic characteristics. Accordingly, the findings should be interpreted not as a definitive design prescription, but as a step toward clarifying the relationships among platform geometry, hydrodynamic coefficients, and dynamic response for semi-submersible floating wind turbine platforms.

Finally, the reported results are limited to the investigated parameter ranges, environmental conditions, and the numerical modeling framework adopted herein. Nevertheless, the findings provide a useful basis for understanding the sensitivity of dynamic responses to design variables and for supporting conceptual design of semi-submersible platforms for floating wind turbine systems. Future work is recommended to employ higher-fidelity fully coupled simulations and advanced CFD-based approaches to further examine effects such as vortex shedding, fluid–structure interaction, and viscous phenomena.

Symbol Definitions for Formulations

M	Effective Mass	f_{ext}	External Force
D	Drag Force	ρ (fluid)	Fluid Density
R	Cross-sectional Radius	a	Acceleration
k	Wave Number	k (restraint)	Stiffness of Restraint
F_H	Horizontal Force	C_o	Yaw Damping
C	Equivalent Damping	L	Lift Force
ρ (air)	Air Density	CD	Drag Coefficient
u	Flow Velocity	CM	Added Mass Coefficient
r	Component Radius	Δx	Lateral Displacement
K_H	Horizontal Stiffness	K	Yaw Spring Stiffness
d_n	Acceleration or Displacement	M (yaw)	Moment of Inertia about Yaw Axis
V	Flow Speed	\ddot{x}	Structure Acceleration
\dot{x}	Structure Velocity	T	Tension Force
A₁	First Order Bessel Function	θ	Angular Velocity
f_{int}	Internal Force	A	Effective Blade Area

References

1- Withee, J. E., (2004). Fully coupled dynamic analysis of a floating wind turbine system (Doctoral dissertation, Monterey California. Naval Postgraduate School).

2- Wayman, E. N. (2006). Coupled Dynamic Modeling of Floating Wind Turbine Systems. Massachusetts Institute of Technology and National Renewable Energy Laboratory. <https://doi.org/10.4043/18287-MS>.

3- Matha, D., Schlipf, M., Pereira, R., & Jonkman, J., (2011), June. Challenges in simulation of aerodynamics, hydrodynamics, and mooring-line dynamics of floating offshore wind turbines. In *ISOPE International Ocean and Polar Engineering Conference*. <https://onepetro.org/ISOPEIOPEC/proceedings-abstract/ISOPE11/All-ISOPE11/12370>.

4- Yang, Y., Bashir, M., Michailides, C., Li, C., & Wang, J., (2020). Development and application of an aero-hydro-servo-elastic coupling framework for analysis of floating offshore wind turbines. *Renewable Energy*, 161, 606-625. <http://dx.doi.org/10.1016/j.renene.2020.07.134>.

5- Xu, K., Gao, Z., & Moan, T., (2019). A study on fully nonlinear wave load effects on floating wind turbine. *Journal of Fluids and Structures*, 88, 216-240. <https://doi.org/10.1016/j.jfluidstructs.2019.05.008>.

6- Li, H., & Bachynski-Polić, E. E., (2021). Validation and application of nonlinear hydrodynamics from CFD in an engineering model of a semi-submersible floating wind turbine. *Marine Structures*, 79, 103054. <https://doi.org/10.1016/j.marstruc.2021.103054>.

7- Ferri, G., Marino, E., & Borri, C., (2020). Optimal dimensions of a semisubmersible floating platform for a 10 MW wind turbine. *Energies*, 13(12), 3092. <https://doi.org/10.3390/en13123092>.

8- Sandua-Fernández, I., Vittori, F., Eguinoa, I., & Cheng, P. W., (2022), November. Impact of hydrodynamic drag coefficient uncertainty on 15 MW floating offshore wind turbine power and speed control. In *Journal of Physics: Conference Series* (Vol. 2362, No. 1). <http://dx.doi.org/10.1088/1742-6596/2362/1/012037>.

9- He, Y. P., Zhao, Y. S., Yang, X. Y., & Zhang, G. R., (2024). Coupled dynamic response analysis of multi-column floating offshore wind turbine with low center of gravity. *Journal of Ocean Engineering and Science*. <http://dx.doi.org/10.1016/j.joes.2022.07.004>.

10- Jonkman, J., & Musial, W., (2010). Offshore code comparison collaboration (OC3) for IEA Wind Task 23 offshore wind technology and deployment (No. NREL/TP-5000-48191). National Renewable Energy Lab (NREL).

11- Hansen, M., (2008). *Aerodynamics of wind turbines*. Routledge.

12- Hansen, M. H., Gaunaa, M., & Madsen, H. A., (2004). A Beddoes-Leishman type dynamic stall model in state-space and indicial formulations. *Risø National Laboratory*.

13- Journée, J. M. J., & Massie, W. W., (2001). *Offshore Hydromechanics*. Delft University of Technology.

14- Morison, J. R., Johnson, J. W., & Schaaf, S. A., (1950). The force exerted by surface waves on piles. *Journal of Petroleum Technology*, 2(05), 149-154. <https://doi.org/10.2118/950149-G>.

15- MacCamy, R. C., & Fuchs, R. A., (1954). Wave forces on piles: a diffraction theory (No. 69). *US Beach Erosion Board*.

16- Hilber, H. M., Hughes, T. J. R., & Taylor, R. L. (1977). Improved numerical dissipation for time integration algorithms in structural dynamics. *Earthquake Engineering & Structural Dynamics*, 5(3), 283–292. <https://doi.org/10.1002/eqe.4290050306>.

17- Simis AS, (2026). *SIMIS* (Version 4) [Computer software]. Simis AS, NTNU spin-off company, Leonardveien 3, NO-7790 Malm, Norway. <https://www.simis.io/>.

18- National Cartographic Center of Iran, (2026). *Bathymetry Map of the Persian Gulf and Gulf of Oman* [Map]. NCC, Tehran, Iran. <https://en.ncc.gov.ir/>.

19- GEBCO Compilation Group, (2023). *GEBCO 2023 Grid*. General Bathymetric Chart of the Oceans. <https://doi.org/10.5285/f98b053b-0cbc-6c23-e053-6c86abc0af7b>.

20- Javidaneh, A., (2023). Director General of National Cartographic Center of Iran (NCC). Retrieved from [ncc.gov](https://en.ncc.gov.ir/Services): <https://en.ncc.gov.ir/Services>.

21- Oceans, g. b., (2023). *Gridded Bathymetry Data-Data & Products - Seabed*. Retrieved from GEBCO: <https://www.gebco.net>.

22- Robertson, A., (2014). Definition of the semisubmersible floating system for phase II of OC4. *NREL Technical Report*, NREL/TP-5000-60601.

23- Chakrabarti, S. K., (1994). *Offshore structure modeling* (Vol. 9). World Scientific. https://www.researchgate.net/publication/238058967_Offshore_Code_Comparison_Collaboration_OC3_for_IEA_Wind_Task_23_Offshore_Wind_Technology_and_Deployment